The sea state bias in altimeter sea level estimates determined by combining wave model and satellite data

N. Tran
CLS/Space Oceanography Division, Ramonville St-Agne, France

D. Vandemark
University of New Hampshire, Durham, NH

S. Labroue
CLS/Space Oceanography Division, Ramonville St-Agne, France

H. Feng
University of New Hampshire, Durham, NH

B. Chapron
Ifremer/Centre de Brest, Plouzané, France

H. L. Tolman
NOAA/NCEP, Camp Springs, MD

J. Lambin
CNES, Toulouse, France

N. Picot
CNES, Toulouse, France

Corresponding author address:
Dr. Ngan Tran, CLS/DOS, 8-10 rue Hermes, 31520 Ramonville St-Agne, France.
E-mail: ntran@cls.fr
Phone: 33-5-61-39-37-22 / Fax: 33-5-61-39-37-82

[Final version of Manuscript for JGR-Ocean, October 2009]

Abstract –

This study documents a method for increasing the precision of satellite-derived sea level measurements. Results are achieved using an enhanced three-dimensional sea state bias (SSB) correction model derived from both Jason-1 altimeter ocean observations (i.e. sea state and wind) and estimates of mean wave period from a numerical ocean wave model, NOAA's WAVEWATCH III. A multi-year evaluation of Jason-1 data indicates sea surface height variance reduction of 1.26 (±0.2) cm^2 in comparison to the commonly applied two-parameter SSB model. The improvement is similar for two separate variance reduction metrics and for separate annual datasets spanning 2002-2004. Spatial evaluation of improvement shows skill increase at all latitudes. Results indicate the new model can reduce the total Jason-1 and Jason-2 altimeter range error budgets by ~7.5%. In addition to the 2D and 3D model differences in correcting the range for wave field variability, mean model regional differences also occur across the globe and indicate a possible 1-2 cm gradient across ocean basins linked to the zonal variation in wave period (short fetch and period in the west, swells and long period in the east). Overall success of this model provides first evidence that operational wave modelling can support improved ocean altimetry. Future efforts will attempt to work within the limits of wave modelling capabilities to maximize their benefit to Jason-1 and Jason-2 sea state bias correction methods.

I. INTRODUCTION

The sea state bias (SSB) in ocean altimetry refers to the cm-level range adjustment applied to improve satellite radar estimation of mean sea level. The first-order SSB predictor, ε, is the height of the dominant gravity waves and can be written as $\varepsilon(m) = \beta * SWH$, where SWH is significant wave height and where β is $O(0.03$ or $3\%)$. Most remaining variability and uncertainty in β resides in a term called the electromagnetic (EM) bias [e.g. Chelton et al., 2001], arising in simplest terms because the radar altimeter power backscattered from wave troughs is enhanced over that from wave crests.

Despite many field observation and modelling efforts, unresolved complexities in the interactions between radar scattering and gravity wave elevation and slope dynamics dictate the continued reliance upon empirical satellite-based SSB estimation to develop the operational models. These empirical formulations have been refined in the past decade using a nonparametric statistical estimation approach [Gaspar et al., 2002], but a recognized limitation is that the correction is solely determined by SWH and surface wind speed (U) data. These two variables are chosen pragmatically because they are readily obtained from the satellite altimeter itself. However, it is expected that SSB uncertainty can be lowered if additional and accurate information on the instantaneous surface wave field are obtained and applied as indicated by several non-satellite field studies [Millet et al., 2003, Melville et al., 2004]. This task is a key remaining challenge for SSB improvement.

This study presents a new multi-dimensional satellite SSB model where ocean wave period data are used within a three-input estimator. The mean gravity wave period (Tm) estimates come from a numerical wind-wave model, NOAA's WAVEWATCH

III (NWW3) [Tolman et al., 2002]. The impetus for this approach stems from recent works examining NWW3 data application to the SSB problem [Feng et al., 2006; Tran et al., 2006]. In particular, Tran et al. [2006] showed that when using global satellite and wave model data, SSB estimation improvement is regionally obtained when using two different wave field statistical parameters. The first is the swell amplitude component of the total sea state (H_{swell}) partitioned using Hanson and Phillips [2001] formulation and the second is the mean wave period defined as

$$Tm = m_0/m_1 \tag{1}$$

$$m_x = \iint S(f, \theta)\, f^{\,x}\, df\, d\theta \tag{2}$$

where m_x represents the respective statistical moments derived from the directional wave elevation density spectrum S (f, θ), with frequency f and wave propagation direction θ. These findings were consistent with studies indicating that wave age, or the overall degree of wave development, measurably impacts the mean wave field steepness and hence the EM bias dynamics [Fu and Glazman, 1991; Minster et al., 1992; Glazman et al., 1996; Chapron et al., 2001; Millet et al., 2003; Melville et al., 2004].

A basic illustration of the Jason-1 altimeter range bias explained by the NWW3 mean wave period using on-orbit data is supplied in Fig. 1. It presents simple bin-averaged values of the altimeter sea level anomaly (SLA) data, without any SSB model correction (see Eq. 4), for a given (SWH, U) data subset with respect to Tm. Results show more than 3 cm of variation (i.e. 1% of SWH) across a wave period range of 6.5-9 s. Since the current working estimate of operational SSB model error is given as O(1%) [Chelton et al., 2001], this finding appears significant. A nearly linear relationship is displayed and the SSB magnitude is much larger for short period (associated to steeper young seas) than for long period (i.e. sinusoidal older seas)

waves.

While Tm is not the sole wave field statistic pertinent to gravity wave impacts on the altimeter electromagnetic bias, this study will focus on removing the observed Tm dependence by developing an empirical multi-dimensional SSB model. The central study objective is to quantify the positive impact that wave model data can have on altimeter sea level data quality by combined use of NWW3 and Jason-1 altimeter data. The new satellite correction model is developed using a known 2D SSB nonparametric estimation approach revised to include three terms (SWH, U, Tm). Its skill will be compared to that of the standard 2D model (i.e. based solely on SWH and U) developed in the same manner and with the same datasets.

II. METHODS

NWW3 was run on a global 1°x1° grid at a 6 hourly time step, without assimilation of altimeter wave height and forced with synoptic winds from the European Centre for Medium-Range Weather Forecasts (ECMWF). Further details about the combined NWW3 / Jason-1 dataset can be found in Tran et al [2006]. Changes in the modelling approach, compared to the one used in the 2006 study include extending the nonparametric statistical model to three dimensions and expanding model validation by adding an assessment that uses collinear (10-day) range measurement differences.

Following Labroue et al. [2004], we derive an on-orbit SSB model from the input data vector **x** using the formulation

$$\varepsilon = \varphi (\mathbf{x}, \theta) \tag{3}$$

where ε is the SSB (in cm), φ is a mapping function, and θ holds the scalar constants for the equation. A kernel smoothing nonparametric approach [Gaspar and Florens, 1998; Gaspar et al., 2002] is used to solve Eq. 3. Following recent studies [Vandemark et al., 2002; Labroue et al., 2004; Tran et al., 2006] we develop a

solution for ε by directly relating the altimeter sea level anomaly (SLA) data, derived from a sea surface height (SSH′) uncorrected for SSB, to input data vector **x** as

$$SLA(\mathbf{x}) = SSH'(\mathbf{x}) - MSL(\mathbf{x}) = \varepsilon(\mathbf{x}) + \sigma(\mathbf{x}). \quad (4)$$

MSL represents the mean sea surface level consisting of a decade-long average [Hernandez and Schaeffer, 2001] that enfolds both the geoid and mean dynamic topography while σ is a noise term combining all standard sea surface height correction errors (e.g. tides, high frequency barotropic effect, ionospheric delay, water vapor, etc..) plus the time-varying sea surface topography. The key assumption of this approach is that under sufficient averaging $\sigma(\mathbf{x}_j)$ will tend to zero for each specific combination (j) of the input variables leaving a direct relationship between the dependent data and ε. In our study, the vector **x** dataset is formed using millions of coincident samples of SWH, U and Tm; the first two variables taken directly from the Jason-1 altimeter and the latter from the wave model data interpolated in space and time to coincide with each altimeter measurement. The extension of a satellite based SSB NP solution to include a third input has not been accomplished before. However, increasing the input vector dimensions is straightforward [e.g. Millet et al., 2003] and primarily requires a computational increase and a sufficiently large amount of measurements. For this study the same local-linear kernel smoothing approach (including kernel and adaptive bandwidth) is kept from Tran et al. [2006] and the model now solved for the 3D vector **x**= (SWH, U, Tm). We developed a solution resulting in a 3D lookup table that describes the SSB behaviour over 0-13 m in SWH, 0-25 m/s in U, and 0-18 sec in Tm. Models were generated using one complete year of data, typically ~16 million samples, for each of the years: 2002, 2003, and 2004. Observed model differences between these solutions are small, below cm levels, and we principally discuss the year 2002 solution in this paper. Next, as a means to the

most direct evaluation of improvement gained by extending the SSB model to higher dimensions, a benchmark 2D SSB algorithm is also computed based on the standard altimeter SWH and U inputs and from the same Jason-1 datasets and using the same NP methods.

Our use of the direct SLA method [Vandemark et al, 2002] as recalled in Eq. 4 does differ from the two alternative SSB approximation approaches. These methods use elevation differences calculated at fixed locations and between two successive satellite measurement times- over the Jason-1 10 day satellite repeat pass period for the collinear approach, and over shorter periods of 3 to 5 days for the satellite pass crossover approach [Labroue et al, 2004]. In these indirect calculation approaches, the relatively short time lapse between t_1 and t_2 and fixed location range differencing allows near isolation of the SSB as follows:

$$\Delta SSH = SSH'_2 - SSH'_1 = \varepsilon(t_2) - \varepsilon(t_1) + \gamma \quad (5)$$

Labroue et al. [2004] evaluates both the direct and indirect (SSH differences) methods to find similar SSB solutions are achieved even though the processes determining if σ and γ tend to zero are not equivalent. Based on that work, either approach is deemed reasonable for this study. Numerically, it is significantly more straightforward to implement the direct approach for NP estimation when including higher dimensional inputs and therefore this study uses the direct method.

The chosen approach for model comparison follows from Tran et al. [2006]. 3D model assessment against 2D and 1D SSB benchmarks will be performed using the recognized standard metric for comparing SSB models, i.e. calculation of the total variance reduction in the derived SSH after application of these specific SSB models. Results are gathered in Table 1. It is recognized that this test and the empirical methods for SSB modelling are each imperfect solutions for model determination and

validation. For example, one disadvantage of the direct SSB model solution is the possibility that data sparseness in certain portions of the 2D and 3D input data domains will lead to ineffective removal of the dynamic topography under averaging in Eq. 4. While a full year of data is deemed adequate to create the direct SSB model for study objectives, we also address such concerns in two ways in the validation. First, the variance reduction metrics are evaluated over several complete-year data sets. This insures independence between the data used in SSB model creation and validation, i.e. the year 2002-version solutions are evaluated not only using 2002 measurements but also with 2003 and 2004 altimeter SSH data. Results from the 2004-version of the models are also provided for comparison. A second step is added both because of the familiarity in the SSB community of working with collinear and crossover differences and to expand confidence in validating this new three-input SLA SSB solution; we include a separate 2D and 3D model SSB assessment of the SSH variance reduction by using Eq. 5 with 10 day repeat pass Jason-1 difference data. This is a variance reduction calculation using the direct SSB model inserted into Eq. 5, not a calculation of yet another SSB model using collinear methods. If one observes relative consistency of results between these metrics then this provides further support that model inaccuracies lie significantly below the level of improvements gained. We note the primary study objective is to provide a method and solution for an improved SSB model and not to attain a final operational model validated under all conditions.

III. RESULTS AND DISCUSSION

Range error related to wind and sea state dynamics as predicted by the new 3D Jason-1 altimeter model is shown in Fig. 2. This model is developed with one year of satellite and model data from year 2002. The corrections are presented as familiar 2D

grids [cf. Gaspar et al., 2002] with contours given in cm. The fixed value of the third parameter for each panel in Fig. 2 is indicated in the caption. Shading denotes the available sample density across each 2D data domain. The left panel can be directly compared to the Jason-1 2D model in Labroue et al. [2004] (their Fig. 9) and agrees closely. The middle and right panels illustrate that SSB also varies systematically with Tm. The middle panel in the data-rich region shows a 3 to 4 cm variation versus Tm at a value of SWH=3.2 m, with bias magnitude decreasing as the wave period increases. This result is consistent with Fig. 1, and an *O*(1%) SWH variation is apparent at most SWH values in the middle panel. Nonlinear variation of the SSB versus dependent variables is evident in all panels and validates the use of the kernel smoothing model approach.

As with previous satellite sea state bias studies, we use altimeter sea surface height variance reduction metrics to assess model performance. The main objective is to determine if the 3D correction model is able to reduce variance in sea level measurements relative to the present-day standard 2D approach. For completeness, we present results from two different validation metrics – 1) variance reduction in the altimeter-derived sea level anomaly using candidate SSB models and 2) variance reduction in the 10-day differenced SSH obtained from along track satellite repeat passes (collinear differences, Eq. 5).

Results for one-year global estimates are provided in Table 1. For both methods, evaluations are performed after applying 1-, 2-, and 3D SSB model corrections. The explained variance is given with respect to a 1D benchmark SSB model [Tran et al., 2006] where positive numbers indicate enhanced magnitude in correction skill (cm^2). The 2D Jason-1 model is built using altimeter SWH and U as discussed earlier. As part of sensitivity tests for this study we have produced SSB

models using one year of data from two separate years (2002 and 2004) and are evaluating them against data in years 2002-2004.

Model enhancement is most clearly seen in Table 1 by examining differences between the 3D and 2D variance reduction. Also provided are the total variance of both SLA and SSH differences without SSB correction and the variance explained by the 1D SSB model as reference marks. The change from 2D to 3D model consistently provides more than 1 cm^2 improvement with values as high as 1.6 cm^2. The improvements are nearly equivalent for SSB models developed using 2002 or 2004 data, with all values agreeing to better than 0.3 cm^2. The same holds for the absolute 2D and 3D SSB reduction values for the 2002 and 2004 models. The largest variability in the 3D-2D difference is from year to year, with 2003 SLA values being smallest, but these values remain above 1 cm^2. The average of the six values based on SLA (1.26 $\pm$0.2 cm^2) translates to 1.12 cm in root mean square (rms) sea level estimate improvement as a result of this new model compared to a model developed using only SWH and U.

Note that differences between the two separate metric estimators across Table 1 (e.g. 2D SSB results across a given row) are assumed to be related to different yearly average of prevalent wind and sea state conditions but also to different mean values of SLA and collinear SSH differences over these three years. Since the interest is on relative SSB model performance within the separate metrics, the comparison results are consistent within each dataset.

Differences between these two variance- reduction metrics were expected since the variance of SLA and the variance of collinear SSH differences do not encompass exactly the same geophysical content. Collinear repeat pass SSH differencing removes some possible correlation between the suite of altimeter

corrections, the dynamic topography, and sea state that are contained in the SLA estimator. Moreover, the absolute rms value at any location is much smaller than for the SLA and the relative SSB correction contributions (2D and 3D) may well differ and be enhanced in the collinear calculations. Table 1 shows that while the relative differences of 2D and 3D SSB impacts versus the 1D benchmark are slightly larger for the collinear versus the SLA metric, the row three average of 3D-2D differences (1.41 vs. 1.26 cm^2) are nearly equal and thus the positive impact of wave period data due to the 3D SSB model is unambiguous in both tests. Overall, while Table 1 data only provide simple single year estimates of performance, one sees that the 3D model consistently indicates positive impact and that results are nearly insensitive to changes in the data period used to train the model. Year to year variation in these results is slightly larger but this is still small (< 0.3 cm^2) compared to the improvement, and a likely source for these dynamics is temporal variability in the actual wind and wave fields in these years.

Fig. 3 expands beyond a single global value to further examine model performance. Results show variance reduction due to 2D and 3D SSB models versus the 1D benchmark with respect to latitude and using year 2004 collinear ΔSSH Jason-1 measurements (from SSB models trained with 2002 data). It is apparent that the 3D model provides an enhanced correction at all latitudes. The improvement often exceeds 1.0 cm^2, especially at high latitudes where SWH values are larger. Comparisons along latitude show that the 3D value is typically a factor of 1.4-1.6 greater than the 2D SSB explained variance. The improvement at all latitudes can be seen as a large improvement compared to any of the candidate 2D SSB models developed in Tran et al. [2006] (cf. their Fig. 4), thus demonstrating that retaining both the SWH and U from the actual altimeter and adding a wave model parameter

into a 3D estimator leads to increased performance.

Results in Fig. 4 further illustrate the impact of Tm in the SSB correction showing a global map of annually-averaged differences between 2D and 3D SSB models, presenting both the mean and variance. Clear spatial patterns emerge. One sees highest positive mean differences can exceed 1 cm along the western edges of the ocean basins while negative values are found to the east. Nearly continuous zonal gradients are apparent across each ocean basin in both the mean and variance differences. We attribute these features to the zonal gradient in mean wave period distributions, with known dominance of long-period swell in the east and limited fetch and shorter-period waves prevailing in the west [Young, 1999; Chen et al, 2002; Tran et al., 2006; Alves, 2006]. This systematic variation in the wave period can be contrasted with the known meridional gradient in both wave height and wind speed where higher wind and waves most frequently occur at highest latitudes.

Results in Fig. 4 also highlight that one possible ramification of this 3D SSB correction would be the alteration of the mean sea surface [Hernandez and Schaeffer, 2001] and mean dynamic topography (MDT) [Rio and Hernandez, 2004] derived using long-term altimetry missions. These altimeter-influenced products assume that the 2D SSB model is accurate and is consistently applied within a multi-year average. Figure 5 provides one slice across the 3D-2D difference map of Fig 4a. Here one sees a nearly linear 1-2 cm difference between the 2D and 3D models across the middle latitude in the North Pacific and North Atlantic driven by Tm variation. A review of recent work attempting to measure the global MDT by combining surface current drifters, geoid measurements, and altimetry [Vossepoel, 2007; Maximenko et al., 2009] has shown: a) zonal SSH gradients are of order 80-200 cm across basin at middle latitudes in the northern hemisphere, and b) error in estimation methods are 4-

5 cm rms in low current regions and 10-15 cm in higher current regions. The 1-2 cm cross basin gradient due to an SSB model change would then be *O*(1-2%) and this would be both in the MDT and in any derived meridional geostrophic current, and translates grossly in an absolute velocity error below 0.2 cm/s. Combining the small impact with the fact that this systematic 1-2 cm SSB effect lies well below the present MDT detection limits suggests these concerns are of second order at this time.

One further means to quantify this study's implication is to insert the average 1.12 cm rms improvement of Table 1 into the overall altimeter measurement error budget. The SSB uncertainty estimate used in these budgets is typically ~1% of SWH which translates to 2.3 cm of uncertainty at the global median SWH value of 2.3 m. While such a single number estimate does not fully enfold the global range of SWH and SSB dynamics that increase with latitude as in Fig. 3, a 1.12 cm reduction applied to 2.3 cm amounts to a 12.6% improvement. Table 1 of Vincent et al. [2003] calculates the Jason-1 altimeter range estimate uncertainty to be 2.95 cm rms at SWH=2 m. This includes ionospheric, atmospheric, and wave corrections. Inserting the SSB improvement into that budget lowers the total mark to 2.73 cm, a ~7.5% improvement in the total range measurement uncertainty budget. Note that use of filtered SWH when computing the SSB correction values in the operational chain would also reduce the amount of range estimate uncertainty coming from the SSB term. Indeed similarly to the dual-frequency ionospheric correction which is filtered over 100 km in the Jason-2 products, the along-track SSB values would be smoother. The SWH filtering could consists in along-track averaging of the 1 Hz SWH data over a 40-100 km (to be determined) ground segment in order to reduce sporadic noise in the SWH data which do not always look physical.

Finally, as another component of this investigation and while not shown here,

a separate 3D SSB model was also developed by replacing Tm with a variable related to the amplitude of swell (H_{swell}) defined as

$$H_{swell} = 4\sqrt{m_0 - \int_{f_{hp}}^{f_4}\int S(f,\theta)\,df\,d\theta} \quad (6)$$

where f_4 = 0.4 Hz and f_{hp} is the spectral frequency just below the wind sea spectral peak at the half power point in the wind sea spectral density [Hanson and Phillips, 2001].

This model was developed in part because of work in Tran et al. [2006] indicating that H_{swell} data is another candidate for improved global scale SSB modelling. The swell-informed 3D model slightly but consistently outperforms this study's Tm 3D model at latitudes below 20^o (improvement of 0.1-0.3 cm^2), but at high latitudes it underperforms and can even revert to 2D model levels. As evident in Table 1, 0.3 cm^2 is also near the confidence level of estimate evaluations. Still, the ubiquity and frequent dominance of swell in the tropics, its modelling, and its impact on the SSB should not be neglected. Future work will look at both higher-dimensional SSB models and the possibility of more regionally focussed corrections. However, in keeping with the objective of this paper, we assert that the comprehensive and robust improvement obtained solely using Tm provides evidence that ocean wave model data, in this case longer wave information related to the mean spectral wavenumber <k>, can be used to improve the precision of altimeter sea level measurements.

IV. CONCLUSION

This study was built under the assumption that the wave-dependent range bias in satellite altimetry can be improved by the inclusion of ocean wave field data taken from a global hindcast model. Mean wave period estimates from the NOAA's

WAVEWATCH III wind-wave prediction system are combined with Jason-1 altimeter sea state and wind speed estimates to develop a new SSB model and quantify its impact. Results show reduced sea surface height variance both at global and regional scale. This is obtained when comparing to the accepted standard two-dimensional altimeter SSB correction that uses only altimeter measurements. Both the 2D and 3D models were produced using the same SLA data (year 2002 or 2004) and nonparametric estimation method to insure clear demonstration of wave model data impacts. Results of Table 1 and Fig. 4 indicate comprehensive improvement with a global 3D SSB model where a single value global variance gain estimate is 1.26 ($\pm$0.2) cm^2, or 1.12 cm in rms. While this value may appear small, the average improvement is of order 0.13% in SWH (the global mode SWH is 2.3 m), a considerable value given that the two parameter model uncertainty is near 1% SWH. Moreover, as each of the precision mission ocean altimeter correction terms are refined, this *O*(1 cm) improvement is comparable to or greater than those recently achieved in revised orbits, water vapor, and high frequency barotropic model modifications [e.g. Beckley et al., 2007; Carrere and Lyard, 2003]. We estimate the improvement at 7.5% in the total range error for the Jason-1 altimeter and this should similarly apply for the presently orbiting Jason-2 altimeter. Perhaps most notably, this study provides a gain in global SSB variance reduction that has not been previously achieved through many attempts that have dealt solely with use of the two altimeter measurements of SWH and U.

There are several caveats to mention and key issues to address in the near future pertaining to this work. First, the error and resolution limitations of wave field estimates taken from a wave model must be recognized. For this study data set, the agreement between altimeter and wave model SWH was better than 0.2 m rms and for

altimeter and model wind speed, better than 1.5 m/s rms. Validation of the full directional spectrum including swell mode amplitudes and directions are much harder to document and those aspects of the model more suspect [cf. Bidlot et al., 2007]. Thus an important near term issue is documenting uncertainty within SSB models and end product SSH data related to wave model uncertainty. And while the SSB approach here is primarily empirical, further sensitivity studies are underway to evaluate optimal use of wave field parameters from WAVEWATCH-III used in 3D and 4D SSB models including the mean wave number and swell field amplitude. Next, the direct or SLA bias determination method requires a significant amount of data increase in the data density (see Fig. 4) to assure model accuracy in data poor areas of the 3D domain. Therefore we are also developing revised numerical inversion methods to handle very large multi-year datasets spanning 2002-2009. Finally, the same methods need to be applied to the Jason-2 and Topex/Poseidon altimeter mission data to insure that this empirically derived SSB approach is applicable to all data sets that are central to the long-term ocean circulation and sea level rise observations that now extend from 1993 onward.

Acknowledgements. The authors wish to thank the two anonymous reviewers who provided valuable comments that lead us to produce a significantly more comprehensive paper than originally submitted. This work was performed within activities supported by the Centre National d'Etudes Spatiales (CNES) in France and the National Aeronautics and Space Administration (NASA).

REFERENCES

[1] Alves, J-H. G. M., Numerical modelling of ocean swell contributions to the global wind-wave climate, Ocean Modellling, 11, 98-122, 2006.

[2] Beckley B. D., F. G. Lemoine, S. B. Luthcke, R. D. Ray, and N. R. Zelenka, A reassessment of global and regional mean sea level trends from TOPEX and Jason-1 altimetry based on revised reference frame and orbits, Geophys. Res. Lett., 10.1029/2007GL030002, 2007.

[3] Bidlot J.-R., J.-G. Li, P. Wittmann, M. Fauchon, H. Chen, J.–M. Lefèvre, T. Bruns, D. Greenslade, F. Ardhuin, N. Kohno, S. Park, M. Gomez, Inter-comparison of operational wave forecasting systems, Proceedings of 10th Int. Workshop of Waves Hindcasting and Forecasting, Hawaii, 2007.

[4] Carrere, L. and F. Lyard, Modeling the barotropic response of the global ocean to atmospheric wind and pressure forcing - comparisons with observations, Geophy. Res Lettters, 30(6), 10.1029/2002GL016473, 2003.

[5] Chapron, B., D. Vandemark, T. Elfouhaily, D. R. Thompson, P. Gaspar, and S. Labroue, Altimeter sea state bias: A new look at global range error estimates, Geophys. Res. Lett., 28(20), 3947-3950, 2001.

[6] Chelton, D. B., J. C. Ries, B. J. Haines, L.-L. Fu, and P. S. Callahan, Satellite altimetry, in Satellite altimetry and Earth Sciences, Ed. Fu L. and Cazenave A., Int. Geophys. Series, 69, 1-131, 2001.

[7] Chen G., B. Chapron, R. Ezraty, and D. Vandemark, A global view of swell and wind sea climate in the ocean by satellite altimeter and scatterometer, J. Atmos. Oceanic Technol., 19, 1849-1859, 2002.

[8] Feng, H., D. Vandemark, Y. Quilfen, B. Chapron, and B. Beckley, Assessment of wind forcing impact on a global wind-wave model using the TOPEX altimeter, Ocean Engineering, 33, 1431-1461, 2006.

[9] Fu, L., and R. Glazman, The effect of the degree of wave development on the sea state bias in radar altimetry measurement, J. Geophys. Res., 96, 829-834, 1991.

[10] Gaspar, P., and J.-P. Florens, Estimation of the sea state bias in radar altimeter measurements of sea level: Results from a new nonparametric method, J. Geophys. Res.,103, 15,803-15,814, 1998.

[11] Gaspar, P., S. Labroue, F. Ogor, G. Lafitte, L. Marchal, and M. Rafanel, Improving nonparametric estimates of the sea state bias in radar altimetry measurements of sea level, J. Atmos. Oceanic Technol., 19, 1690-1707, 2002.

[12] Glazman, R., A. Fabrikant, M. Srokosz, Numerical analysis of the sea state bias for satellite altimetry, J. Geophys. Res., 101, 3789-3799, 1996.

[13] Hanson, J. L., and Phillips, O.M., Automated analysis of ocean surface directional wave spectra, J. Atmos. Oceanic Technol., 18, 277-293, 2001.

[14] Hernandez F., and P. Schaeffer, The CLS01 Mean Sea Surface: A validation with the GSFC00.1 surface, CLS technical note, pp. 14, 2001. (available at: http://www.aviso.oceanobs.com/fileadmin/documents/data/produits/auxiliaires/cls01_valid_mss.pdf).

[15] Labroue S., P. Gaspar, J. Dorandeu, O.Z. Zanife, F. Mertz, P. Vincent, and D. Choquet, Non-parametric estimates of the sea state bias for Jason-1 radar altimeter, Mar. Geod., 27, 453-481, 2004.

[16] Maximenko N., P. Niiler, M.-H. Rio, O. Melnichenko, L. Centurioni, D. Chambers, V. Zlotnicki, and B. Galperin., Mean dynamic topography of the ocean derived from satellite and drifting buoy data using three different techniques, in

press in J. Atmos. Oceanic Technol. with with proof available at the journal website, 2009.

[17] Melville, W. K., F. C. Felizardo., P. Matusov, Wave Slope and Wave Age Effects in Measurements of Electromagnetic Bias, J. Geophys. Res., 109(C7), 7018, doi: 10.1029/2002JC001708, 2004.

[18] Millet, F. W., D. V. Arnold, K. F. Warnick, and J. Smith, Electromagnetic bias estimation using in situ and satellite data: 1. RMS wave slope, J. Geophys. Res., 108(C2), 3040, doi:10.1029/2001JC001095, 2003.

[19] Minster, J. F., D. Jourdan, C. Boissier, and P. Midol-Monnet, Estimation of the sea state bias in radar altimeter Geosat data from examination of frontal systems, J. Atmos. Oceanic Technol., 9, 174187, 1992.

[20] Rio M.-H and F. Hernandez, A mean dynamic topography computed over the world ocean from altimetry, in situ measurements, and a geoid model, *J. Geophys. Res.*, 109, C12032, doi:10.1029/2003JC002226, 2004.

[21] Tolman, H. L., B. Balasubramaniyan, L. D. Burroughs, D. V. Chalikov, Y. Y. Chao, H. S. Chen, and V. M. Gerald, Development and implementation of wind generated ocean surface wave models at NCEP, Weather and Forecasting, 17, 311-333, 2002.

[22] Tran N., D. Vandemark, B. Chapron, S. Labroue, H. Feng, B. Beckley, and P. Vincent, New models for satellite altimeter sea state bias correction developed using global wave model data, J. Geophys. Res., 111, C09009, doi:10.1029/2005JC003406, 2006.

[23] Vandemark, D., N. Tran, B. D. Beckley, B. Chapron, and P. Gaspar, Direct estimation of sea state impacts on radar altimeter sea level measurements. Geophys. Res. Lett., 29(24), 2148. doi :10.1029/2002GL015776, 2002.

[24] Vincent P., S. D. Desai, J. Dorandeu, M. Ablain, B. Soussi, P. S. Callahan, and B. J. Haines, Jason-1 geophysical performance evaluation, Marine Geodesy, 26, 167-186, 2003.

[25] Vossepoel F. C., Uncertainties in the mean ocean dynamic topography before the launch of the Gravity Field and Steady-State Ocean Circulation Explorer (GOCE), *J. Geophys. Res.*, 112, C05010, doi:10.1029/2006JC00389, 2007.

[26] Young, I. R., Seasonal variability of the global ocean wind and wave climate, Int. J. Climatol., 19, 931-950, 1999.

FIGURE CAPTIONS

Fig. 1. Average altimeter sea state bias estimates versus mean wave period determined from Jason-1 SLA observations (without application of SSB correction) where SWH is fixed at 3.2 m (± 0.1) and U is fixed at 9.5 ms^{-1} (± 1.0). The result includes 156,200 samples from 2002-2004 and 95% confidence intervals are shown. A normalized probability density function for the mean wave period (dashed line) is also provided.

Fig. 2. New 3D Jason-1 SSB estimator as a function of SWH, U, and Tm. This is shown using three 2D arrays with the respective third variable held constant. From left to right, these fixed values are Tm = 8.4 s, U = 9.5 m/s, and SWH = 3.2 m. Isopleths represent a given SSB value (units in cm). Shaded areas represent data density with darkest gray holding no data, medium gray: less than 20 samples, lighter shade less than 100, and the white region exceeding 100 samples per bin. The model is produced using all data in the year 2002.

Fig. 3. Variation with latitude of band-averaged SSH variance (cm^2) reduction (positive values) obtained using the 2D and 3D models in comparison to a 1D (-3.8% SWH) benchmark. Results are obtained by collinear analyses for year 2004 and derived using 10 degree latitude bands.

Fig. 4. Maps of (a) annual average of the difference (2D-3D) between the two models (in cm), and (b) variance difference (3D-2D) between the models.

Fig. 5. Annual average of SSB estimate differences between the 2 models across the North Pacific and North Atlantic at about 39°N (extracted from Fig 4.a). They are compared with mean wave period Tm variation.

TABLE CAPTION

Table 1. The magnitude of variance reduction obtained with the common 2D and the new 3D SSB correction models relative to the reduction obtained when applying a 1D SSB correction (-3.8% SWH). Each estimate is for a full year of global Jason-1 altimeter data. The results are calculated using both the Jason-1 SLA and collinear (10-day) SSH difference data sets for the years indicated. Models were developed using year 2002 or 2004 data as indicated. Also provided are the total variance of both SLA and SSH differences without (w/o) SSB correction and the variance explained by the 1D SSB model.

Jason-1 sea state bias models		Relative sea level anomaly variance reduction (cm^2)			Relative collinear ΔSSH variance reduction (cm^2)		
		Validation dataset			Validation dataset		
		2002	2003	2004	2002	2003	2004
2002 version	2D SSB	1.37	1.62	1.88	2.80	2.98	3.20
	3D SSB	2.83	2.65	3.26	4.18	4.51	4.82
	Difference (3D – 2D)	1.46	1.03	1.38	1.38	1.53	1.62
2004 version	2D SSB	1.32	1.72	2.06	2.79	2.97	3.26
	3D SSB	2.47	2.74	3.56	3.89	4.33	4.74
	Difference (3D – 2D)	1.15	1.02	1.50	1.10	1.36	1.48
		SLA w/o SSB			collinear ΔSSH w/o SSB		
Total Variance (cm^2)		120.99	121.08	118.72	82.22	83.97	81.90
Variance explained by 1D SSB (cm^2)		22.55	23.48	21.88	18.94	18.37	17.24

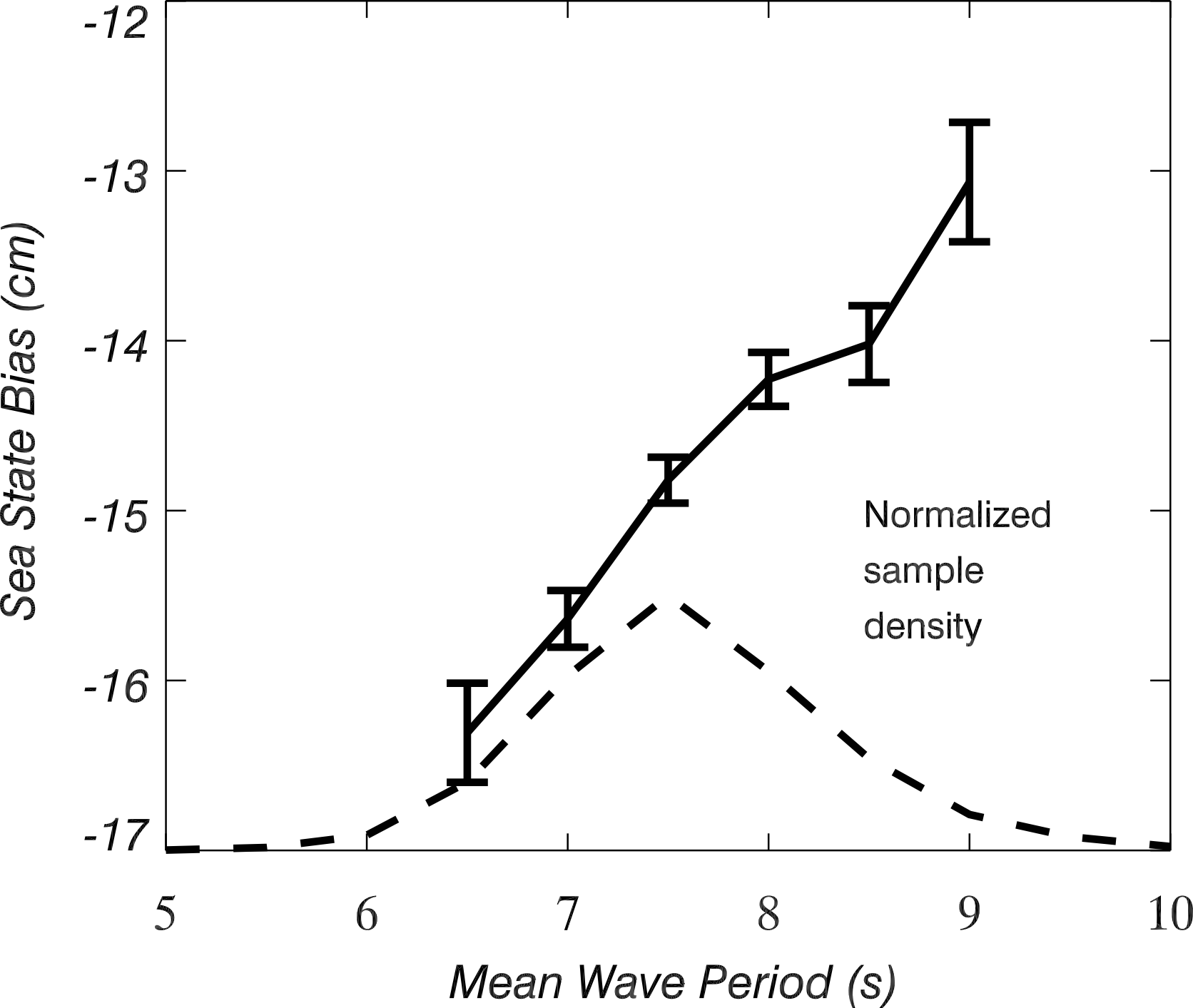
-12
-13
-14
-15
-16
-17
Sea State Bias (cm)
5
6
7
8
9
10
Mean Wave Period (s)
Normalized
sample
density

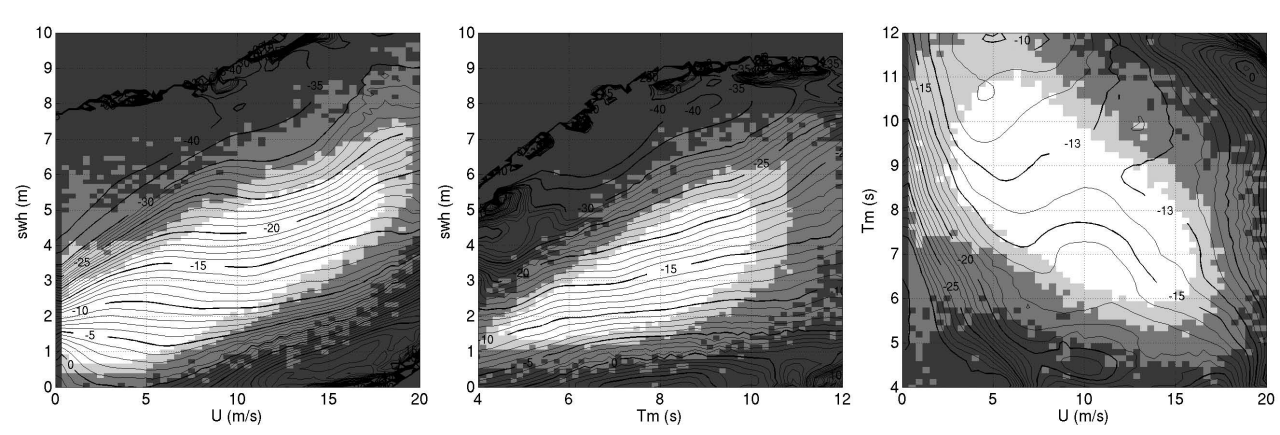
swh (m)
U (m/s)
swh (m)
Tm (s)
Tm (s)
U (m/s)

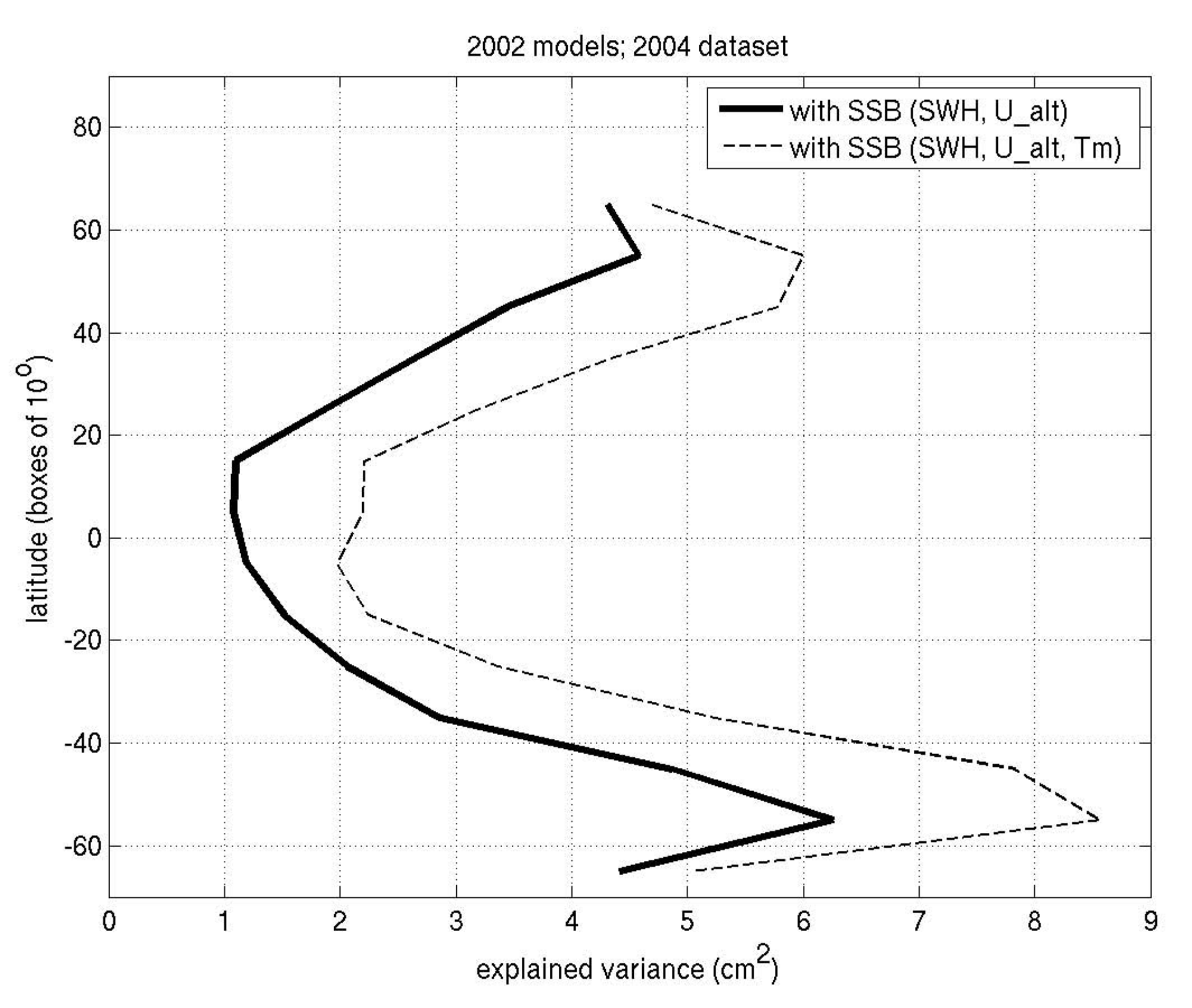
2002 models; 2004 dataset
with SSB (SWH, U_alt)
with SSB (SWH, U_alt, Tm)
latitude (boxes of 10^o)
80
60
40
20
0
-20
-40
-60
0
1
2
3
4
5
6
7
8
9
explained variance (cm^2)

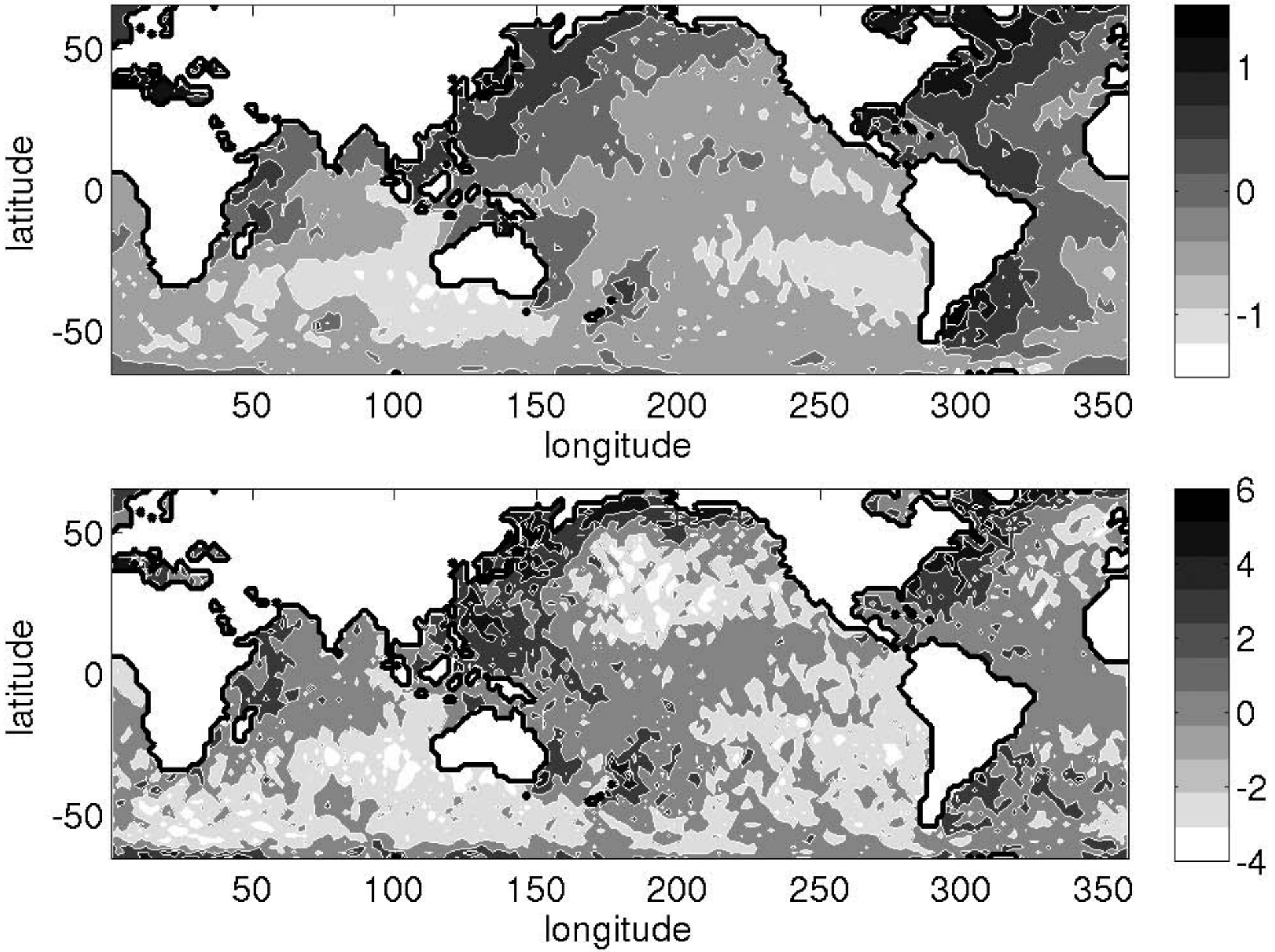
50
0
-50
latitude
50
100
150
200
250
300
350
longitude
1
0
-1
6
4
2
0
-2
-4

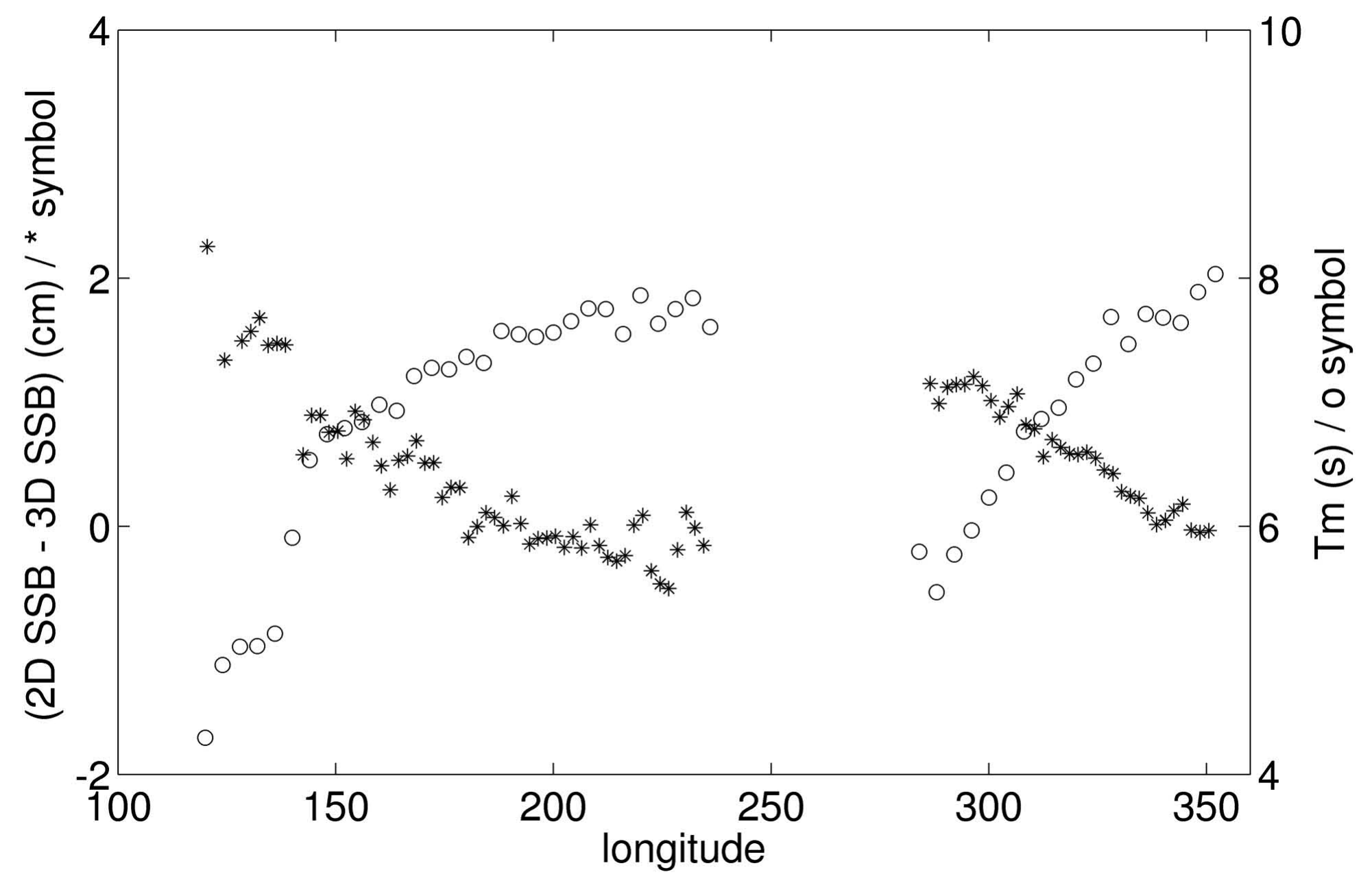
4
2
0
-2
10
8
6
4
100
150
200
250
300
350
longitude
(2D SSB - 3D SSB) (cm) / * symbol
Tm (s) / o symbol